

Unitarity constraints and role of geometrical effects in deep–inelastic scattering and vector–meson electroproduction

S. M. Troshin and N. E. Tyurin

*Institute for High Energy Physics,
Protvino, Moscow Region, 142280, Russia*

Abstract

Deep–inelastic scattering at low Bjorken x and elastic vector meson electroproduction are analyzed on the basis of the off-shell s –channel unitarity. We discuss behavior of the total cross–section of virtual photon–proton scattering and obtain, in particular, that the exponent in the power-like dependence of σ_p^{tot} is related to the interaction radius of a constituent quark. The explicit mass dependence of the exponent in the power energy behavior of the vector meson electroproduction has been obtained. Angular distributions at large momentum transfers are considered. The energy dependence of the total cross–section of γp –interactions is also obtained.

Introduction

Rising dependence of the virtual photon–proton scattering total cross–section on the center of mass energy \bar{W}^2 discovered at HERA [1] led to the renewed interest in the mechanism of diffraction at high energies. Such behavior was in fact predicted in [2] and expected in perturbative QCD [3]. The HERA effect is consistent with various \bar{W}^2 – dependencies and has been explained in the different ways, among them is a manifestation of hard BFKL Pomeron [4], an appearance of the DGLAP evolution in perturbative QCD [3], a transient phenomena, i.e. preasymptotic effects [5] or a true asymptotical dependence of the off–mass–shell scattering amplitude [6]. There is an extensive list of papers devoted to this subject and many interesting results are described in the review papers (cf. e.g. [1, 7]). The strong rise which can be described by the power-like dependence ¹

$$\sigma_p^{\text{tot}}(\bar{W}^2; Q^2) / (\bar{W}^2)^{\alpha(Q^2)} \quad (1)$$

with $\alpha(Q^2)$ rising with Q^2 from about 0.1 to 0.4 is a somewhat surprising fact since according to our knowledge of energy dependence of the total cross–sections in hadronic interactions, the total cross–section increase is rather slow ($\alpha \approx 0.1$). However the above difference is not a fundamental one. First, there is no Froissart–Martin bound for the case off–shell particles [2, 6]. Only under some additional assumptions this bound can be applied [9, 10]. Second, it cannot be granted that the preasymptotic effects and approach to the asymptotics are the same for the on–shell and off–shell scattering. It seems that for some unknown reasons scattering of virtual particles reaches the asymptotics faster than the scattering of the real particles. It is worth noting that the space-time structure of the low– x scattering involves large distances $1 - 1 = x$ on the light–cone [11], and the region of $x \approx 0$ is sensitive to the nonperturbative contributions. Deep–inelastic scattering in this region turns out to be a coherent process where diffraction plays a major role and nonperturbative models such as Regge or vector dominance model can be competitive with perturbative QCD and successfully applied for description of the experimental data.

It is essential to obey the general principles in the nonperturbative region and, in particular, to satisfy unitarity. The most common form of unitarity solution – the eikonal one – was generalized for the off–shell scattering in [6]. In this paper we consider off–shell extension of the U –matrix approach to the amplitude unitarization. It is shown that this approach along with the respective extension of the chiral quark model for the U –matrix [12] leads to (1), where the exponent $\alpha(Q^2)$ is related to the Q^2 –dependent interaction radius attributed to constituent

¹There are other parameterizations which describe the experimental data equally well (cf. e.g. [8]).

quark. These results cannot be reproduced in the eikonal form which provides naked “Born” form (with nonleading corrections) for the output amplitude in the case of the off-shell scattering [6]. The fundamental difference between the two forms of the amplitude unitarization lies in the analytical properties in the complex energy plane [13].

It is worth noting here importance of the effective interaction radius concept [14]. The study of the effective interaction radius dependence on the scattering variables appeared to be very useful for understanding of the dynamics of high energy hadronic reactions [15, 16]. It is widely known nowadays that the respective geometrical considerations provide a deep insight in hadron dynamics and deep-inelastic scattering (cf. [17]).

Besides the studies of deep-inelastic scattering (DIS) at low x the interesting measurements of the characteristics of the elastic vector meson (VM) production were performed in the experiments H1 and ZEUS at HERA [18, 19]. It was shown that the integral cross section of the elastic vector meson production increases with energy in the way similar to the $\sigma_p^{\text{tot}}(W^2; Q^2)$ dependence on W^2 [1]. It appeared that an increase of VM electroproduction cross-section with energy is steeper for heavier vector mesons as well as when the virtuality Q^2 is higher. Discussion of such a behavior in various model approaches based on the nonperturbative hadron physics or perturbative QCD can be found in (cf. e.g. [7]).

Application of approach based on the off-shell extension of the s -channel unitarity to elastic vector meson electroproduction $\gamma^* p \rightarrow V p$ allows to obtain angular dependence and predict interesting mass effects in these processes. It appears that the obtained mass and Q^2 dependencies are in agreement with the experimentally observed trends and again the results differ from the eikonal unitarization, where the cross-section of these processes does not exceed the Froissart–Martin bound [6]. It is also valid for the angular distributions at large momentum transfers.

1 Off-shell unitarity

Extension of the U -matrix unitarization for the off-shell scattering was considered in [9]. To apply an extended unitarity to DIS at small x there was supposed that the virtual photon fluctuates into a quark–antiquark pair $q\bar{q}$ and this pair was treated as an effective virtual vector meson state in the processes with small x . This effective virtual meson interacts then with a hadron. We considered a single effective vector meson field and used for the amplitudes of the processes

$$V + h \rightarrow V + h; \quad V + h \rightarrow V + h \quad \text{and} \quad V + h \rightarrow V + h \quad (2)$$

the notations $F(s; t; Q^2)$, $F(s; t; Q^2)$ and $F(s; t)$ respectively, i. e. we denoted in that way the amplitudes when both initial and final mesons are off mass shell, only initial meson is off mass shell and both mesons are on mass shell.

The unitarity relation for the amplitudes F and F has a similar structure as the unitarity equation for the on-shell amplitude F but relates different amplitudes. In impact parameter representation at high energies it relates the amplitudes F and F in the following way

$$\text{Im}F(s; b; Q^2) = \mathcal{F}(s; b; Q^2) \mathcal{f} + \mathcal{G}(s; b; Q^2); \quad (3)$$

where $\mathcal{F}(s; b; Q^2)$ is the contribution to the unitarity of many-particle intermediate on-shell states. The function $\mathcal{G}(s; b; Q^2)$ is the sum of the n-particle production cross-section in the process of the virtual meson interaction with a hadron h, i. e.

$$\mathcal{G}(s; b; Q^2) = \sum_n \mathcal{G}_n(s; b; Q^2);$$

There is a similar relation for the functions F and F ,

$$\text{Im}F(s; b; Q^2) = F(s; b; Q^2)F(s; b; Q^2) + \mathcal{G}(s; b; Q^2); \quad (4)$$

Contrary to $\mathcal{G}(s; b; Q^2)$ the function $\mathcal{G}(s; b; Q^2)$ has no simple physical meaning and it will be discussed later.

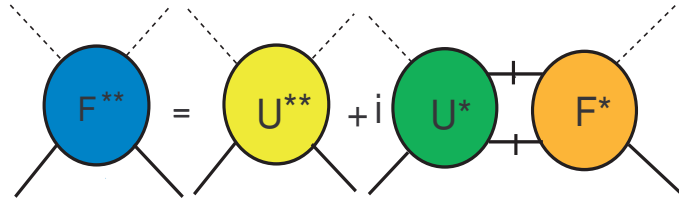


Figure 1: The solution of the off-shell unitarity relation for the amplitude F .

The solution of the off-shell unitarity relations can be graphically represented for the amplitude F and F in the Figs. 1 and 2 respectively and has a simple form in the impact parameter representation [9]:

$$\begin{aligned} F(s; b; Q^2) &= U(s; b; Q^2) + iU(s; b; Q^2)F(s; b; Q^2) \\ F(s; b) &= U(s; b; Q^2) + iU(s; b; Q^2)F(s; b); \end{aligned} \quad (5)$$

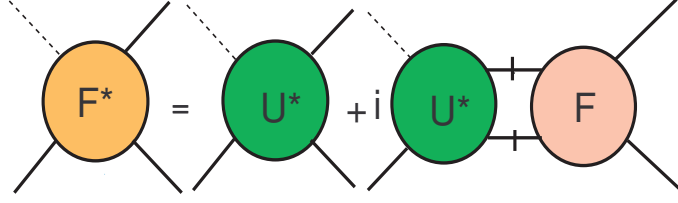


Figure 2: The solution of the off-shell unitarity relation for the amplitude F .

It is worth noting that the solution of the off-shell unitarity in the nonrelativistic case for a K -matrix representation was obtained for the first time in [20]. The solution of this system has a simple form when the factorization is assumed

$$[U(s; b; Q^2)]^2 - U(s; b; Q^2)U(s; b) = 0: \quad (6)$$

Eq. (6) implies the following representation for the functions U and U :

$$\begin{aligned} U(s; b; Q^2) &= \mathcal{I}^2(s; b; Q^2)U(s; b) \\ U(s; b; Q^2) &= \mathcal{I}(s; b; Q^2)U(s; b): \end{aligned} \quad (7)$$

It is valid, e. g. in the Regge model with factorizable residues and the Q^2 -independent trajectory. It is also valid in the off-shell extension of the chiral quark model for the U -matrix which we will consider further. Thus, we have for the amplitudes F and F

$$F(s; b; Q^2) = \frac{U(s; b; Q^2)}{1 - iU(s; b)} = \mathcal{I}(s; b; Q^2) \frac{U(s; b)}{1 - iU(s; b)} \quad (8)$$

$$F(s; b; Q^2) = \frac{U(s; b; Q^2)}{1 - iU(s; b)} = \mathcal{I}^2(s; b; Q^2) \frac{U(s; b)}{1 - iU(s; b)} \quad (9)$$

and unitarity provides inequalities

$$|F(s; b; Q^2)| \leq |\mathcal{I}(s; b; Q^2)| |F(s; b; Q^2)| \leq |\mathcal{I}^2(s; b; Q^2)| |F(s; b; Q^2)| \quad (10)$$

It is worth noting that the above limitations are much less stringent than the limitation for the on-shell amplitude $|F(s; b)| \leq 1$.

When the function $\mathcal{I}(s; b; Q^2)$ is real we can write down a simple expression for the inelastic overlap function $\mathcal{I}(s; b; Q^2)$:

$$\mathcal{I}(s; b; Q^2) = \mathcal{I}^2(s; b; Q^2) \frac{\text{Im}U(s; b)}{1 - iU(s; b)} \quad (11)$$

The following relation is valid for the function $\mathcal{U}(s; b; Q^2)$:

$$\mathcal{U}(s; b; Q^2) = [\mathcal{U}(s; b; Q^2) \mathcal{U}(s; b)]^{1=2} : \quad (12)$$

Eq. (12) allows one to connect the integral

$$\mathcal{U}(s; Q^2) = \int_0^1 \mathcal{U}(s; b; Q^2) b db$$

with the total inelastic cross-section:

$$\mathcal{U}(s; Q^2) \int_0^1 b db = \sigma_{inel}(s) :$$

2 Off-shell scattering in the U-matrix method

In this section we consider off-shell extension of the model for hadron scattering [12], which uses the notions of chiral quark models. Valence quarks located in the central part of a hadron are supposed to scatter in a quasi-independent way by the effective field. In accordance with that we represent the basic dynamical quantity in a factorized form. In the case when one of the hadrons (vector meson in our case) is off mass shell the off-shell U-matrix, i.e. $\mathcal{U}(s; b; Q^2)$ is represented as the product

$$\mathcal{U}(s; b; Q^2) = \prod_{i=1}^{\mathcal{Y}^h} \mathcal{H}_{Q_i}(s; b) \prod_{j=1}^{\mathcal{Y}^v} \mathcal{H}_{Q_j}(s; b; Q^2) : \quad (13)$$

Factors $\mathcal{H}_{Q_i}(s; b)$ and $\mathcal{H}_{Q_j}(s; b; Q^2)$ correspond to the individual quark scatterings smeared over transverse position of the constituent quark inside hadron and over fraction of longitudinal momentum of the initial hadron carried by this quark. Under the virtual constituent quarks Q we mean the ones composing the virtual meson. Factorization (13) reflects the coherence in the valence quark scattering and may be considered as an effective implementation of constituent quarks' confinement. The picture of hadron structure with the valence constituent quarks located in the central part and the surrounding condensate implies that the overlapping of hadron structures and interaction of the condensates occur at the first stage of the collision. Due to an excitation of the condensates, the quasiparticles, i.e. massive quarks arise (cf. Fig. 3).

These quarks play role of scatterers. To estimate number of such quarks one could assume that part of hadron energy carried by the outer condensate clouds is being released in the overlap region to generate massive quarks. Then their number can be estimated by the quantity:

$$N(s; b) / \frac{(1 - k_Q^2)^{p-s}}{m_Q} D_c^h = D_c^v ; \quad (14)$$

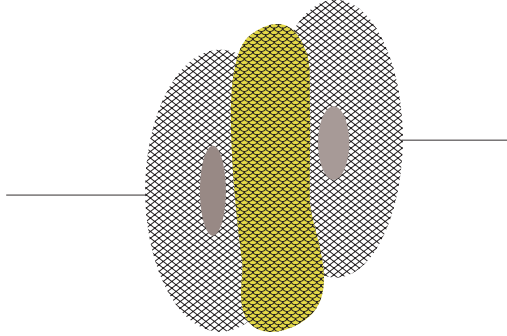


Figure 3: Schematic view of an initial stage of the hadron interaction and formation of the effective field.

where m_Q – constituent quark mass, k_Q – hadron energy fraction carried by the constituent valence quarks. Function D_c^h describes condensate distribution inside the hadron h , and b is an impact parameter of the colliding hadron h and meson V . Thus, $N(s; b)$ quarks appear in addition to $N = n_h + n_V$ valence quarks. Those quarks are transient ones: they are transformed back into the condensates of the final hadrons in elastic scattering. It should be noted that we use subscript Q to refer the constituent quark Q and the same letter Q is used to denote a virtuality Q^2 . However, they enter formulas in a way excluding confusion.

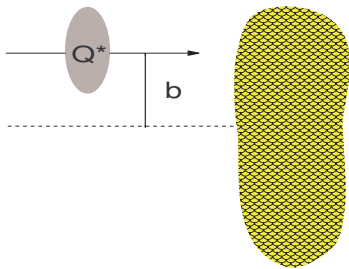


Figure 4: Schematic view of the virtual constituent quark Q scattering in the effective field generated by $N_{sc}(s; b)$ scatterers, where $N_{sc}(s; b) = N(s; b) + N - 1$.

The amplitudes $\langle f_Q(s; b) \rangle$ and $\langle f_Q(s; b; Q^2) \rangle$ describe elastic scattering of a single valence on-shell Q or the off-shell Q quarks with the effective field (cf.

Fig. 4) and we use for the function $hf_Q(s; b)$ the following expression

$$hf_Q(s; b) = [N(s; b) + (N - 1)]V_Q(b) \quad (15)$$

where $V_Q(b)$ has a simple form $V_Q(b) / g \exp(-m_Q b)$, which corresponds to the quark interaction radius $r_Q = 1/m_Q$. The function $hf_Q(s; b; Q^2)$ is to be written as

$$hf_Q(s; b; Q^2) = [N(s; b) + (N - 1)]V_Q(b; Q^2) \quad (16)$$

In the above equation

$$V_Q(b; Q^2) = g(Q^2) \exp(-m_Q b(Q^2)) \quad (17)$$

and this form corresponds to the virtual constituent quark interaction radius

$$r_Q = 1/m_Q(Q^2) \quad (18)$$

Introduction of the Q^2 dependence into the interaction radius of constituent quark constituent quark which in the present approach consists of a current quark and the cloud of quark-antiquark pairs of the different flavors [12] is the main issue of the model and the origin of this dependence and possible physical interpretation will be discussed in Section 6.

The b -dependence of $N(s; b)$ is weak compared to the b -dependence of V_Q or V_Q [12] and therefore we have taken this function to be independent on the impact parameter b . Dependence on virtuality Q^2 comes through dependence of the intensity of the virtual constituent quark interaction $g(Q^2)$ and the $1/m_Q(Q^2)$, which determines the quark interaction radius (in the on-shell limit $g(Q^2) \rightarrow g$ and $1/m_Q(Q^2) \rightarrow 1/m_Q$). According to these considerations the explicit functional forms for the generalized reaction matrices U and U can easily be written in the form of (7) with

$$hf_Q(s; b; Q^2) = \frac{hf_Q(s; b; Q^2)}{hf_Q(s; b)} \quad (19)$$

Note that (6) and (7) imply that the amplitude of the process $Q \rightarrow Q$ is the following

$$hf_{Q \rightarrow Q}(s; b; Q^2) = [hf_Q(s; b; Q^2)]^2 [hf_Q(s; b)]^{1-2} \quad (20)$$

We consider the high-energy limit and for the simplicity assume here that all the constituent quarks have equal masses and parameters g and $1/m_Q$ as well as $g(Q^2)$

and $\mathcal{G}(Q^2)$ do not depend on quark flavor. We also assume for the simplicity pure imaginary amplitudes. Then the functions U , U and U are the following

$$U(s; b) = i g^N \frac{s}{m_Q^2} \exp \left[-\frac{m_Q N b}{Q^2} \right] \quad (20)$$

$$U(s; b; Q^2) = \mathcal{G}(b; Q^2) U(s; b); \quad U(s; b; Q^2) = \mathcal{G}^2(b; Q^2) U(s; b) \quad (21)$$

where the function \mathcal{G} is an energy-independent one and has the following dependence on b and Q^2

$$\mathcal{G}(b; Q^2) = \frac{g(Q^2)}{g} \exp \left[-\frac{m_Q b}{Q^2} \right] \quad (22)$$

with

$$\mathcal{G}(Q^2) = \frac{g(Q^2)}{g} \quad (23)$$

3 Total cross-sections of p and n interactions

It is obvious that for the on-shell particles $W^2 = 1$ and we arrive to the result obtained in [9] at large W^2

$$\sigma_p^{\text{tot}}(W^2) / \frac{2}{m_Q^2} \ln^2 \frac{W^2}{m_Q^2}; \quad (24)$$

where the usual for DIS notation W^2 instead of s is used. Similar result is valid also for the off mass shell particles when the interaction radius of virtual quark does not depend on Q^2 and is equal to the interaction radius of the on-shell quark, i.e. $\mathcal{G}(Q^2) = 1$. The behavior of the total cross-section at large W^2

$$\sigma_p^{\text{tot}}(W^2) / \frac{g(Q^2)}{g m_Q} \ln^2 \frac{W^2}{m_Q^2}; \quad (25)$$

corresponds to the result obtained in [9]. We consider further the off-shell scattering with $\mathcal{G}(Q^2) \neq 1$ and it should be noted first that for the case when $\mathcal{G}(Q^2) < 1$ the total cross-section would be energy-independent

$$\sigma_p^{\text{tot}}(W^2) / \frac{g(Q^2)}{g(Q^2) m_Q} \ln^2 \frac{W^2}{m_Q^2}$$

in the asymptotic region. This scenario would mean that the experimentally observed rise of σ_p^{tot} is transient preasymptotic phenomena [5, 9]. It can be realized when we replace in the formula for the interaction radius of the on-shell constituent quark $r_Q = r_{m_Q}$ the mass m_Q by the value $m_Q = \sqrt{m_Q^2 + Q^2}$ in order to obtain the interaction radius of the off-shell constituent quark and write it down as $r_Q = r_{m_Q}$, or equivalently replace r_{m_Q} by $r_{m_Q}(Q^2) = r_{m_Q} \sqrt{m_Q^2 + Q^2}$. The above option cannot be excluded in principle, however, it is a self-consistent choice in the framework of the model only at large $Q^2 \gg m_Q^2$ since it was originally supposed that the function r_{m_Q} is universal for the different quark flavors.

However, when $r_{m_Q}(Q^2) > r_{m_Q}$ the situation is different and we have at large W^2

$$\sigma_p^{\text{tot}}(W^2; Q^2) / G(Q^2) = \frac{W^2}{m_Q^2} \ln \frac{W^2}{m_Q^2}; \quad (26)$$

where

$$r_{m_Q}(Q^2) = \frac{r_{m_Q}(Q^2)}{r_{m_Q}}; \quad (27)$$

We shall further concentrate on this self-consistent for any Q^2 values and the most interesting case.

All the above expressions for $\sigma_p^{\text{tot}}(W^2)$ can be rewritten as the corresponding dependencies of $F_2(x; Q^2)$ at small x according to the relation

$$F_2(x; Q^2) = \frac{Q^2}{4} \sigma_p^{\text{tot}}(W^2);$$

where $x = Q^2/W^2$.

In particular, (26) will appear in the form

$$F_2(x; Q^2) / G(Q^2) = \frac{1}{x} \ln(1/x); \quad (28)$$

It is interesting that the value and Q^2 dependence of the exponent $r_{m_Q}(Q^2)$ is related to the interaction radius of the virtual constituent quark. The value of parameter r_{m_Q} in the model is determined by the slope of the differential cross-section of elastic scattering at large t [21], i. e.

$$\frac{d}{dt} / \exp \frac{2}{m_Q N} P - t \quad (29)$$

and from the pp-experimental data it follows $r_{m_Q} = 2 \pm 0.5$. The uncertainty is related to the ambiguity in the constituent quark mass value. Using for simplicity

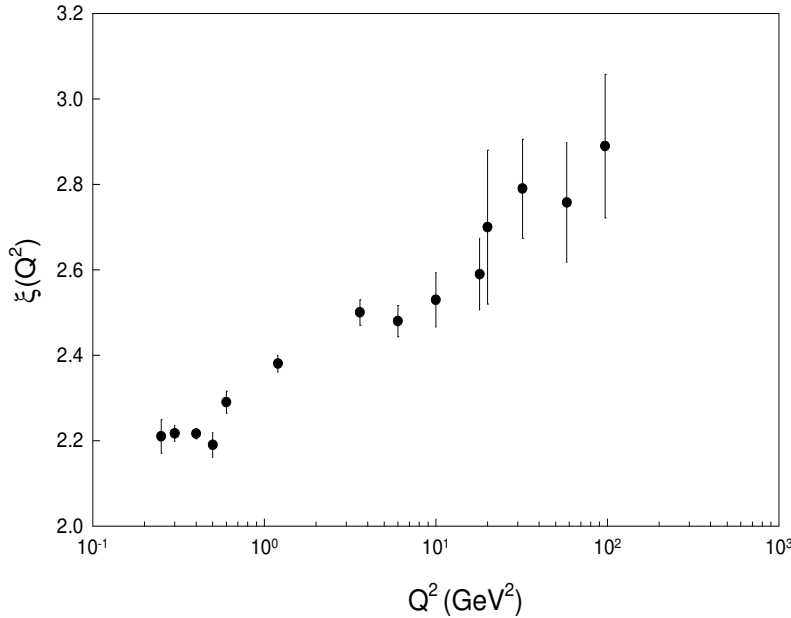


Figure 5: The “experimental” behavior of the function $\xi(Q^2)$.

$\xi(Q^2) = 2$ and the data for $\xi(Q^2)$ obtained at HERA [17] we calculated the “experimental” Q^2 -dependence of the function $\xi(Q^2)$:

$$\xi(Q^2) = \frac{2}{1 - \ln(Q^2)} \quad (30)$$

The results are represented in Fig. 5. It is clear that experiment leads to $\xi(Q^2)$ rising with Q^2 . This rise is slow and consistent with $\ln Q^2$ extrapolation. Thus, assuming this dependence to be kept at higher Q^2 and using (27), we predict saturation in the Q^2 -dependence of $\xi(Q^2)$, i.e. at large Q^2 the flattening will take place. This rise corresponds to the increasing interaction radius of the constituent quarks from the virtual vector meson (Fig. 6).

The extension of the above approach to the calculation of the total cross-section is straightforward. The following behavior of the total cross-section at large W^2 will take place:

$$\sigma_{\text{tot}}(W^2; Q_1^2; Q_2^2) / G(Q_1^2)G(Q_2^2) \sim \frac{W^2}{m_Q^2} \ln \frac{W^2}{m_Q^2} \quad (31)$$

Such strong energy dependence of the total cross-section is consistent with LEP data [22].

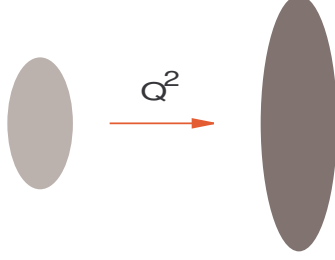


Figure 6: The increase with virtuality of the constituent quark interaction radius.

4 Elastic vector meson production

As it was already mentioned we assumed that the virtual photon before the interaction with the proton fluctuates into the $Q\bar{Q}$ pair and for simplicity we limited ourselves with light quarks under discussion of the total cross-section. The expression for the total cross-section is given by (26). The calculation of the elastic and inelastic cross-sections can also be directly performed in this approximation using (20), (21) and (22) and integrating over impact parameter (8) and (11). Then we obtain the following dependencies for the cross-sections of elastic scattering and inelastic interactions

$$\sigma_p^{el}(W^2; Q^2) / G_e(Q^2) = \frac{W^2}{m_Q^2} \ln \frac{W^2}{m_Q^2} \quad (32)$$

and

$$\sigma_p^{inel}(W^2; Q^2) / G_i(Q^2) = \frac{W^2}{m_Q^2} \ln \frac{W^2}{m_Q^2} \quad (33)$$

with the universal exponent $\ln \frac{W^2}{m_Q^2}$ given by the Eq. (27). The above relations mean that the ratios of elastic and inelastic cross-sections to the total one do not depend on energy.

Now we consider elastic (exclusive) cross-sections both for light and heavy vector mesons production. We need to get rid of the light quark limitation and extend the above approach in order to include the quarks with the different masses. The inclusion, in particular, heavy vector meson production into this scheme is straightforward: the virtual photon fluctuates before the interaction with proton into the heavy quark-antiquark pair which constitutes the virtual heavy vector meson state. After the interaction with a proton this state turns out into the real heavy vector meson.

Integral exclusive (elastic) cross-section of vector meson production in the process $p \rightarrow V p$ when the vector meson in the final state contains not necessarily light quarks can be calculated directly according to the above scheme and formulas of Section 2:

$$\sigma_p^V(W^2; Q^2) / G_V(Q^2) = \frac{W^2}{m_Q^2} \sigma_V(Q^2) \ln \frac{W^2}{m_Q^2}; \quad (34)$$

where

$$\sigma_V(Q^2) = (Q^2) \frac{m_Q}{m_Q^2}; \quad (35)$$

In (35) m_Q denotes the mass of the constituent quarks from the vector meson and m_Q^2 is the mean constituent quark mass of system of the vector meson and proton system. Evidently $\sigma_V(Q^2) = (Q^2)$ for the light vector mesons. This result is consistent with the most recent ZEUS data, but statistics is still limited [18]. In the case when the vector meson is very heavy, i.e. $m_Q \gg m_Q$ we have

$$\sigma_V(Q^2) = \frac{5}{2} (Q^2);$$

We conclude that the respective cross-section rises faster than the corresponding cross-section of the light vector meson production, e.g. (35) results in

$$\sigma_{J=1}(Q^2) \sim 2 (Q^2);$$

This is in a qualitative agreement with the recently observed trends in the HERA data [19].

5 Angular structure of elastic and proton-dissociative vector meson production

Recently the first measurements of angular distributions at large t in the light vector meson production were performed [23] and it was found that angular distribution is consistent with the power dependence $(-t)^3$ in the proton-dissociative processes [24].

We apply the model described above for calculation of the differential cross-sections in elastic vector meson production using an analysis of the singularities of the amplitudes in the complex impact parameter plane developed in [21].

Since the integration goes over the variable b^2 rather than b it is convenient to consider the complex plane of the variable b^2 where $b^2 = b^2$ and analyze singularities in the b^2 -plane. Using (8) we can write down the integral over the contour C

around a positive axis in the s -plane:

$$F(W^2; t; Q^2) = \frac{W^2}{2} \int_C F(W^2; ; Q^2) K_0\left(\frac{P}{t}\right) d; \quad (36)$$

where K_0 is the modified Bessel function and the variable W^2 was used instead of the variable s . The contour C can be closed at infinity and the value of the integral will be then determined by the singularities of the function $F(W^2; ; Q^2)$, where

$$F(W^2; ; Q^2) = ! (; Q^2) \frac{U(W^2;)}{1 - iU(W^2;)}$$

in a s -plane.

With explicit expressions for the functions U and $!$ we conclude that the positions of the poles are

$$s_n(W^2) = \frac{2}{M^2} \ln g^N \frac{W^2}{m_Q^2} + i n g^2; \quad n = 1; 3; \dots$$

where $M = m_Q n_v + m_Q n_h$. The location of the poles in the complex impact parameter plane does not depend on the virtuality Q^2 . Besides the poles $F(W^2; ; Q^2)$ has a branching point at $s = 0$ and

$$\text{disc } F(W^2; ; Q^2) =$$

$$\frac{\text{disc}[!(; Q^2)U(W^2;)] - iU(W^2; + i0)U(W^2; - i0)\text{disc}!(; Q^2)}{[1 - iU(W^2; + i0)][1 - iU(W^2; - i0)]};$$

i.e.

$$\text{disc } F(W^2; ; Q^2) \sim i \text{disc}!(; Q^2)$$

since at $W^2 \rightarrow 1$ the function $U(W^2;) \rightarrow 1$ at fixed s . The function $F(W^2; t; Q^2)$ can be then represented as a sum of pole and cut contributions, i.e.

$$F(W^2; t; Q^2) = F_p(W^2; t; Q^2) + F_c(W^2; t; Q^2):$$

The pole and cut contributions are decoupled dynamically when $W^2 \rightarrow 1$. Contribution of the poles determines the amplitude $F(W^2; t; Q^2)$ in the region $W^2 \rightarrow 1$ and it can be represented in a form of series:

$$F(W^2; t; Q^2) \sim \sum_{n=1; 3; \dots}^X \exp\left(\frac{i n}{N} v(Q^2)\right) \frac{P}{n} K_0\left(\frac{P}{t_n}\right); \quad (37)$$

At moderate values of τ when $\tau \approx 1$ (GeV/c) the amplitude (37) leads to the Orear type behavior of the differential cross-section which is similar to the Eq.(29) for the on-shell amplitude, i.e.

$$\frac{d_v}{dt} \sim \exp \left[-\frac{2}{M} p \tau \right] ; \quad (38)$$

At small values of τ the behavior of the differential cross-section is complicated. The oscillating factors $\exp \left[\frac{i n}{N} v(Q^2) \right]$ which are absent in the on-shell scattering amplitude [12] play a role.

At large τ the poles contributions is negligible and contribution from the cut at $\tau = 0$ is a dominating one. It appears that the function $F_c(W^2; \tau; Q^2)$ does not depend on energy and differential cross section depends on τ in a power-like way

$$\frac{d_v}{dt} \sim G(Q^2) \tau^{-3} ; \quad (39)$$

Therefore for large values of τ ($\tau \approx m_Q^2 = Q^2$) we have a simple $(\tau)^{-3}$ dependence of the differential cross-section. This dependence significantly differs from the one in the on-shell scattering [12] which approximates the quark counting rule [25] and this difference is in the large extent because of the off-shell unitarity role.

It is to be noted that the ratio of the two differential cross-sections for the production of the vector mesons V_1 and V_2 does not depend on the variables W^2 and τ at large enough values of τ .

The production of the vector mesons accompanied by the proton dissociation into the state Y with mass M_Y can be calculated along the lines described in [26] with account for non-zero virtuality. The extension is straightforward. Similar to the case of on-shell particles we have a suppression of the pole contribution at high energies. It is interesting to note that the normalized differential cross-section

$$\frac{1}{\sigma_0(W^2; M_Y^2; Q^2)} \frac{d}{dt dM_Y^2}$$

where σ_0 is the value of cross-section at $\tau = 0$ will exhibit a scaling behavior

$$\frac{1}{\sigma_0} \frac{d}{dt dM_Y^2} = \tau^{-3} ; \quad (40)$$

where the \mathcal{M} is the following combination

$$\mathcal{M}(Q^2) = M_Y \left[1 - \frac{2m_Q}{M_Y} (Q^2) \right] ; \quad (41)$$

Note that $M(Q^2) \sim M_Y$ at small values of Q^2 or when the value of M_Y is large $M_Y \sim m_Q$. The dependence (40) is in agreement with the experimentally observed dependencies in the proton-dissociative vector meson production at large values of t .

There are different approaches to the vector meson production, e.g. recent application of the geometrical picture was given in [27]. Angular distributions can be described also in the approaches based on the perturbative QCD [28] which provide smooth power-like t -dependence. Brief review of the recent results of these approaches can be found in [29].

6 Impact parameter picture

The results described above rely on the off-shell unitarity and Q^2 -dependence of the constituent quark interaction radius. It is useful to consider an impact parameter picture to get insight into the physical origin of this Q^2 -dependence. Impact parameter analysis of the experimental data is, in particular, a tool for the detection of unitarity effects in hadronic reactions [30] and diffractive DIS [31]. In the present study impact parameter profile of the amplitude is peripheral when (Q^2) increases with Q^2 (Fig. 7). The dependence on virtuality of constituent quark interaction radius was assumed and this assumption has appeared to be consistent with the experimental data. It was demonstrated then that the rising dependence of the constituent quark interaction radius with virtuality is in good agreement with the experimental data which indicate the rising Q^2 -dependence of the exponent (Q^2) . The relation (27) between (Q^2) and (Q^2) implies a saturation in the Q^2 -dependence of (Q^2) at large values of Q^2 . The reason for increase

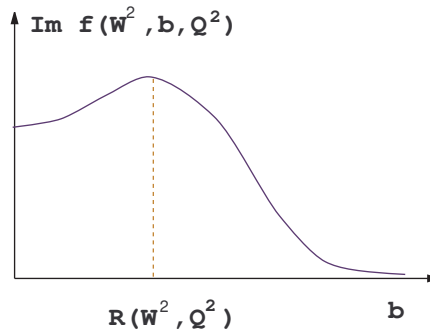


Figure 7: The impact parameter profile of the scattering amplitude.

of the constituent quark interaction radius with virtuality should have a dynamical nature and it could originate from the emission of the additional $q\bar{q}$ -pairs in

the nonperturbative structure of a constituent quark. In the present approach constituent quark consists of a current quark and the cloud of quark–antiquark pairs of the different flavors [12]. It was shown that the available experimental data imply a $\ln Q^2$ –dependence of the radius of this cloud.

The peripheral profile of the amplitude in its turn can result from the increasing role of the orbital angular momentum of the quark–antiquark cloud when the virtual particles are considered. The generation of $q\bar{q}$ -pairs cloud could be considered in analogy with the theory of superconductivity. It was proposed [32] to push further this analogy and consider an anisotropic extension of the theory of superconductivity which seems to match well with the above nonperturbative picture for a constituent quark. The studies [33] of that theory show that the presence of anisotropy leads to axial symmetry of pairing correlations around the anisotropy direction $\hat{\Gamma}$ and to the particle currents induced by the pairing correlations. In other words it means that a particle of the condensed fluid is surrounded by a cloud of correlated particles (“hump”) which rotate around it with the axis of rotation $\hat{\Gamma}$. Calculation of the orbital momentum shows that it is proportional to the density of the correlated particles.

7 Conclusion

We considered limitations the unitarity provides for the p –total cross-sections and geometrical effects in the model dependence of σ_p^{tot} . In particular, it was shown that the Q^2 –dependent constituent quark interaction radius can lead to a nontrivial, asymptotical result: $\sigma_p^{\text{tot}} \sim (W^2)^2 (Q^2)$, where (Q^2) will be saturated at large values of Q^2 . This result is valid when the interaction radius of the virtual constituent quark is rising with virtuality Q^2 . The data for the structure functions at low values of x continue to demonstrate the rising total cross-section of p –interactions and therefore we can consider it as a reflection of the rising with virtuality interaction radius of a constituent quark.

The steep energy increase of total cross-section $\sigma_p^{\text{tot}} \sim (W^2)^2 (Q^2)$ was also predicted. In elastic vector meson electroproduction processes the mass and Q^2 dependencies of the integral cross-section of vector meson production are related to the dependence of the interaction radius of the constituent quark Q on the respective quark mass m_Q and virtuality Q^2 . The behavior of the differential cross-sections at large τ is in the large extent determined by the off-shell unitarity effects. The smooth power-like dependence on τ is predicted which is in agreement with the experimental data [18]. The new experimental data will be essential for the discrimination of the model approaches and studies of the interplay between the non-perturbative and perturbative QCD regimes (cf. e.g. [17, 27]).

Acknowledgements

We are grateful to J. A. Crittenden for the communications on the ZEUS experimental data on the angular distributions and A. Borissov for the discussions of the HERMES experimental data. We would also like to thank M. Islam, E. Martynov, V. Petrov and A. Prokudin for many interesting discussions of the results.

References

- [1] A. M. Cooper-Sarkar, R. C. E. Devenish and A. De Roeck, *Int. J. Mod. Phys. A* **13**, 3385 (1998).
- [2] C. Lopez and F. J. Yndurain, *Phys. Rev. Lett.* **44**, 1118 (1980).
- [3] V. N. Gribov and L. N. Lipatov, *Sov. J. Phys.* **15**, 438, 625 (1972);
L. N. Lipatov, *Sov. J. Nucl. Phys.* **20**, 94 (1975);
Yu. L. Dokshitzer, *Sov. Phys. JETP* **46**, 641 (1977);
G. Altarelli and G. Parisi, *Nucl. Phys. B* **426**, 298 (1977).
- [4] L. N. Lipatov, *Sov. J. Nucl. Phys.* **23**, 338 (1976);
E. A. Kuraev, L. N. Lipatov and V. S. Fadin, *Sov. Phys. JETP* **45**, 199 (1977);
Y. Y. Balitsky and L. N. Lipatov, *Sov. J. Nucl. Phys.* **28**, 822 (1978).
- [5] P. M. Nadolsky, S. M. Troshin and N. E. Tyurin, *Z. Phys. C* **69**, 131 (1995).
- [6] V. A. Petrov, *Nucl. Phys. Proc. Suppl.* **54A**, 160 (1997);
V. A. Petrov and A. V. Prokudin, *Proceedings of the International Conference on Elastic and Diffractive Scattering, Protvino, Russia, 28 June - 2 July 1999*, p.95, World Scientific, 2000, V. A. Petrov and A. V. Prokudin, eds.
- [7] P. V. Landshoff, hep-ph/0010315;
A. Donnachie, J. Gravelis and G. Shaw, hep-ph/0101221;
S. Munier, A. M. Stařto and A. H. Mueller, hep-ph/0102291.
- [8] G. Wolf, hep-ex/0105055.
- [9] S. M. Troshin and N. E. Tyurin, *Europhys. Lett.* **37**, 239 (1997).
- [10] A. L. Ayala, M. B. Gay Ducati and E. M. Levin, *Phys. Lett. B* **388**, 188 (1996);
A. Capella, E. G. Ferreira, C. A. Salvado and A. B. Kaidalov, hep-ph/0005049.
- [11] E. A. Paschos, *Phys. Lett. B* **389**, 383 (1996);
W. L. van Neerven, *Nucl. Phys. B, Proc. Suppl.* **79**, 36 (1999).
- [12] S. M. Troshin and N. E. Tyurin, *Nuovo Cim.* **106A**, 327 (1993); *Phys. Rev. D* **49**, 4427 (1994).

- [13] R. Blankenbecler and M. L. Goldberger, Phys. Rev. **126**, 766 (1962).
- [14] A. A. Logunov, M. A. Mestvirishvili, Nguen Van Hieu and O. A. Khrustalev, Nucl. Phys. B **10**, 692 (1969).
- [15] T. T. Chou and C. N. Yang, Phys. Rev. **170**, 1591 (1968).
- [16] O. A. Khrustalev, V. I. Savrin and N. E. Tyurin, Comm. JINR E2-4479, 1969.
- [17] A. M. Staśto, K. Golec-Biernat and J. Kwieciński, hep-ph/0007192;
J. Bartels and H. Kowalski, hep-ph/0010345.
- [18] ZEUS Collaboration, J. Breitweg et al., Paper 439 submitted to the XXXth International Conference on High Energy Physics, July27 - August 2, 2000, Osaka, Japan.
- [19] R. Ioshida, hep-ph/0102262 and references therein.
- [20] C. Lovelace, Phys. Rev. **135**, B 1225 (1964).
- [21] S. M. Troshin and N. E. Tyurin, Theor. Math. Phys. **50**, 150 (1982).
- [22] A. De Roeck, hep-ph/0101076.
- [23] ZEUS Collaboration, J. Breitweg et al., Paper 442 submitted to the XXX International Conference on High Energy Physics, 27 July - 2 August, 2000, Osaka, Japan.
- [24] J. A. Crittenden, hep-ex/0010079, references therein and private communication.
- [25] V. A. Matveev, R. M. Muradyan and A. N. Tavkhelidze, Lett. Nuovo. Cim. **7**, 719 (1973)
S. Brodsky and G. Farrar, Phys. Rev. Lett. **31**, 1153 (1973).
- [26] S. M. Troshin and N. E. Tyurin, hep-ph/0008274.
- [27] A. C. Caldwell and M. S. Soares, hep-ph/0101085.
- [28] D. Yu. Ivanov, Phys. Rev. **D53**, 3564;
D. Yu. Ivanov, R. Kirschner, A. Schaäfer and L. Szymanowski, Phys. Lett, **B478**, 101, 2000;
J. R. Forshaw and G. Poludniowski, hep-ph/0107068
- [29] M. Diehl, hep-ph/0109040.
- [30] U. Amaldi and K. R. Schubert, Nucl. Phys. **B166**, 301 (1980).
- [31] B. Povh, B. Z. Kopeliovich and E. Predazzi, Phys. Lett. **B405**, 361 (1997).
- [32] S. M. Troshin and N. E. Tyurin, Phys. Rev. **D52**, 3862, (1995); *ibid.* **D54**, 838, (1996); Phys. Lett. **B355**, 543, (1995).

- [33] P. W. Anderson and P. Morel, Phys. Rev. **123**, 1911, (1961);
F. Gaitan, Annals of Phys. **235**, 390, (1994);
G. E. Volovik, Pisma v ZhETF, **61**, 935, (1995).